

Lateral Macrobicyclic Architectures: Toward New Lead(II) Sequestering Agents

David Esteban-Gómez, Raquel Ferreirós, Susana Fernández-Martínez, Fernando Avecilla, Carlos Platas-Iglesias, Andrés de Blas,* and Teresa Rodríguez-Blas*

Departamento de Química Fundamental e Industrial, Universidade da Coruña, Campus da Zapateira, s/n, 15071 A Coruña, Spain

Received December 20, 2004

The macrobicyclic receptor L^5 derived from 4,13-diaza-18-crown-6 incorporating a pyridinyl Schiff-base spacer, forms stable complexes with lead(II) in the presence of different counterions. The coordination environment of the guest lead(II) ion may be modulated by external factors thanks to the optimal cavity size of L^5 as well as the nature and distribution of its donor atoms. Both in solution and in solid state, the guest lead(II) is nearly centered into the macrobicyclic cavity of L^5 when poorly coordinating groups such as perchlorate are present. The long Pb–donor atom distances found in the X-ray crystal structure of $[Pb(L^5)](ClO_4)_2 \cdot 0.5H_2O$ (**1**) reveal that weak interactions between the lead(II) ion and the donor atoms of the receptor exist. 1H and ^{207}Pb NMR spectroscopy studies demonstrate that monoprotonation of the receptor L^5 moves the lead(II) ion to one end of the cavity, whereas its diprotonation causes the demetalation of the complex without receptor destruction. This demetalation process is reversible and very fast. All of this, together with the inertia of the receptor toward hydrolysis, opens very interesting perspectives for the use of receptor L^5 as a new lead(II) extracting agent. The X-ray crystal structure of compound $[Pb(HL^5)(NO_3)][Pb(NO_3)_4]$ (**3**) appears to be a good model for the monoprotonated intermediate of the demetalation process. In **3** the lead(II) ion is six-coordinate and clearly placed at one end of the macrobicyclic cavity, which results in a substantial shortening of the bond distances of the lead(II) coordination sphere.

Introduction

As a result of decades of industrial production and use, heavy metal contamination of soils and aquifers is becoming increasingly common at many hazardous waste sites and so studies focused on metal ion removal from both aqueous solutions and soils have become of increasing importance in recent years. In particular, nowadays, lead continues being as one of the most important pollutants.¹ This is one of oldest metals known to man, as well as one of the most useful due to its abundance and its physical properties. The major industrial uses have been for electric storage batteries, paint pigments, gasoline additives, pipes, ammunition, solder, etc. Although the awareness of its environmental and health effects has led to the substitution of lead and lead compounds by alternative materials, the concentration in drinking water, diets, and ambient air may be significant in some areas.² Most lead compounds are insoluble in vivo, so only small

amounts of lead are absorbed from the gastrointestinal tract of adults, but children can absorb up to 50% of ingested lead. Moreover, since it is slowly eliminated, lead accumulates in liver, kidneys, bones, and other parts of the body.³ In the divalent state lead binds preferentially to thiol and phosphate groups in nucleic acids, proteins, and cell membranes^{4–6} originating severe neurological and/or hematological effects.^{7,8}

The most commonly used treatment methods for heavy metal-containing waste presently include precipitation, solvent extraction, activated carbon adsorption, treatment with ion-exchange resins, and bioremediation, whereas other methods less widely used include reverse osmosis, electroly-

(3) Sigel, H.; Da Costa, C. P.; Martín, R. B. *Coord. Chem. Rev.* **2001**, *219–221*, 435.

(4) Sigel, H.; Fischer, B. E.; Farkas, E. *Inorg. Chem.* **1983**, *22*, 925.

(5) Tajmir-Riahi, H. A.; Langlais, M.; Savoie, R. *Nucleic Acids Res.* **1988**, *16*, 751.

(6) Abu-Dari, K.; Hahn, F. E.; Raymond, K. N. *J. Am. Chem. Soc.* **1990**, *112*, 1519.

(7) Goyer, R. A. In *Handbook on Toxicity of Inorganic Compounds*; Seiler H. G., Sigel, H., Sigel A., Eds.; Marcel Dekker: New York, 1988.

(8) Jaffe, E. K.; Volin, M.; Mayers, C. B. *Biochemistry* **1994**, *33*, 11554.

* Authors to whom correspondence should be addressed. E-mail: mayter@udc.es (T.R.-B.); ucambv@udc.es (A.d.B.).

(1) Lanphear, B. P. *Science* **1998**, *281*, 1617.

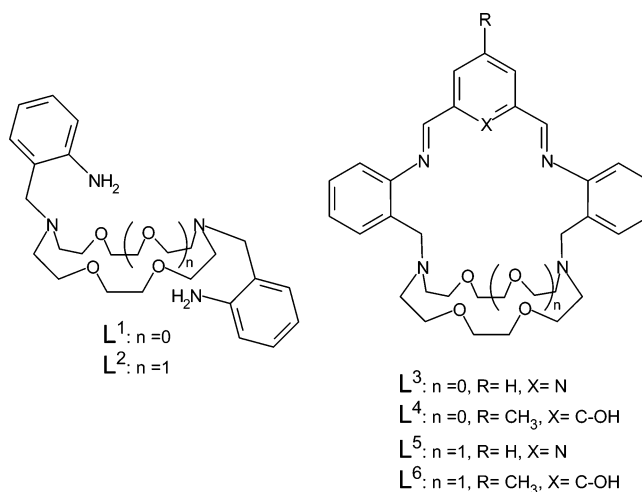
(2) Lanphear, B. P.; Roghmann, K. J. *Environ. Res.* **1997**, *74*, 67.

sis, cementation, irradiation, zeolite adsorption, evaporation, membrane processes, or ion flotation.⁹ When extracting agents are used to remove metal ions from wastewater, the following conditions must be met: fast binding of the metal ion by the complexant agent; selective ion complexation; high binding strength for the metal ion to be extracted; high stability against hydrolysis; reversible complexation allowing for total recovery of the metal without significant extracting agent destruction.¹⁰ Because of the highly favored complexation due to the chelate and macrocyclic effects, chelate and macrocyclic ligands have been widely used for metal extractions. The search for novel highly selective extracting agents for lead has caused a resurgence of interest in the coordination chemistry of Pb(II),¹¹ and in recent years numerous reports concerning coordination chemistry of lead(II) with chelating ligands,¹² macrocycles,^{13–15} lariat ethers,^{16–18} and cryptands¹⁹ have been published.

In this contribution, we report a novel generation of sequestering agents structurally pertaining to the group of receptors described as Schiff-base lateral macrobicycles.²⁰ Taking into account the peculiar structural characteristics of lateral macrobicycles, it is easy to understand that they may exhibit a range of interesting and potentially useful molecular recognition properties. However, only a few studies concerning these molecular architectures have been reported. These studies have revealed that lateral macrobicycles behave as very versatile receptors that can be used as platforms to obtain homo- and heterometallic dinuclear complexes with many different aims (i.e. to induce processes of “push–pull” dimetallic substrate activation)²¹ and as receptors for organic molecules²² or contact ion pairs.^{23,24}

Schiff-base lateral macrobicycles **L**³–**L**⁶ (Chart 1) can be easily prepared in high yields by a template reaction of the corresponding diamine (**L**¹ or **L**², Chart 1) and dialdehyde

Chart 1



precursors (diformylpyridine or diformylphenol).^{25,26} From a structural point of view these receptors derive from the parent azacrowns 1,10-diaza-15-crown-5 (**L**³ and **L**⁴) or 4,13-diaza-18-crown-6 (**L**⁵ and **L**⁶). The presence of these crown moieties into the backbone of our receptors confers them a certain degree of flexibility that is however limited by the presence of a relatively rigid chelate subunit containing a pyridine or phenol group conjugated with two benzyl units through the two imine spacers. In previous works we have carried out studies to assess the different complexation capabilities of the lateral macrobicycles **L**³ and **L**⁶ toward lead(II) ion.^{27,28} As a continuation of these works herein we discuss the ability and potential of **L**⁵ to act not only as a good receptor for lead but also as a sequestering agent for this metal ion. New solid-phase extracting agents derived from this receptor may be developed by covalent attachment of it onto the surface of an organic polymer or silica gel.

Experimental Section

Chemicals and Starting Materials. *N,N'*-Bis(2-aminobenzyl)-1,10-diaza-15-crown-5 (**L**¹), [BaL⁵](ClO₄)₂, and Pb(**L**³)(ClO₄)₂ were prepared as previously described.^{25,27,29} 2,6-Diformylpyridine was prepared according to literature methods.^{30,31} All other chemicals were purchased from commercial sources and used without further purification. Solvents were of reagent grade purified by the usual methods.

Caution! *Although we have experienced no difficulties with the perchlorate salts, these should be regarded as potentially explosive and handled with care.*³²

- (9) Jordanov, A. T.; Roundhill, D. M. *Coord. Chem. Rev.* **1998**, *170*, 93.
(10) Deratani, A.; Seville, B. *Anal. Chem.* **1981**, *53*, 1742.
(11) Parr, J. *Polyhedron* **1997**, *16*, 551.
(12) Harrowfield, J. M.; Miyamae, H.; Skelton, B. W.; Soudi, A. A.; White, A. H. *Aust. J. Chem.* **1996**, *49*, 1067.
(13) Star, A.; Goldberg, I.; Fuchs, B. *Angew. Chem., Int. Ed.* **2000**, *39*, 2685–2689.
(14) Arranz, P.; Bazzicalupi, C.; Bencini, A.; Bianchi, A.; Ciattini, S.; Fornasari, P.; Giorgi, C.; Valtancoli, B. *Inorg. Chem.* **2001**, *40*, 6383 and references therein.
(15) Hancock, R. D.; Shaikjee, M. S.; Dobson, S. M.; Boeyens, J. C. *Inorg. Chim. Acta* **1988**, *154*, 229.
(16) Damu, K. V.; Hancock, R. D.; Wade, P. W.; Boeyens, J. C. A.; Billing, D. G.; Dobson, S. M. *J. Chem. Soc., Dalton Trans.* **1991**, 293.
(17) Liu, L. K.; Lin, C.-S.; Young, D.-S.; Shyu, W.-J.; Ueng, C.-H. *Chem. Commun.* **1996**, 1255.
(18) Inoue, Y.; Gokel, G. W., Eds. *Cation Binding by Macrocycles*; Marcel Dekker: New York, 1990. Gokel, G. W. *Crown Ethers and Cryptands*; The Royal Society of Chemistry: Cambridge, U.K., 1991.
(19) Drew, M. G. B.; Howarth, O. W.; Morgan, G. G.; Nelson, J. *J. Chem. Soc., Dalton Trans.* **1994**, 3149.
(20) Nobel Prize winner J.-M. Lehn described for the first time the term *lateral macrobicyclic* to refer to a molecular architecture resulting from the bridging of a chelate subunit over a macrocycle: Lehn, J.-M. *Pure Appl. Chem.* **1980**, *52*, 2441.
(21) Carroy, A.; Lehn, J.-M. *J. Chem. Soc., Chem. Commun.* **1986**, 1232.
(22) Flack, S. S.; Chaumette, J.-L.; Kilburn, J. D.; Langley, G. J.; Webster, M. *J. Chem. Soc., Chem. Commun.* **1993**, 399.
(23) Mahoney, J. M.; Beatty, A. M.; Smith, B. D. *J. Am. Chem. Soc.* **2001**, *123*, 5847.
(24) Smith, B. D.; Lambert, T. N. *Chem. Commun.* **2003**, 2261.

- (25) Esteban, D.; Bañobre, D.; Bastida, R.; de Blas, A.; Macías, A.; Rodríguez, A.; Rodríguez-Blas, T.; Fenton, D. E.; Adams, H.; Mahía, J. *Inorg. Chem.* **1999**, *38*, 1937.
(26) Platas-Iglesias, C.; Esteban, D.; Ojea, V.; Avecilla, F.; de Blas, A.; Rodríguez-Blas, T. *Inorg. Chem.* **2003**, *42*, 4299.
(27) Esteban, D.; Bañobre, D.; de Blas, A.; Rodríguez-Blas, T.; Bastida, R.; Macías, A.; Rodríguez, A.; Fenton, D. E.; Adams, H.; Mahía, J. *Eur. J. Inorg. Chem.* **2000**, 1445.
(28) Esteban, E.; Avecilla, F.; Platas-Iglesias, C.; Mahía, J.; de Blas, A.; Rodríguez-Blas, T. *Inorg. Chem.* **2002**, *41*, 4337.
(29) Rodríguez-Infante, C.; Esteban, D.; Avecilla, F.; de Blas, A.; Rodríguez-Blas, T.; Mahía, J.; Macedo, A. L.; Geraldés, C. F. G. C. *Inorg. Chim. Acta* **2001**, *317*, 190.
(30) Papadopoulos, E. P.; Jarrar, A.; Issidorides, C. H. *J. Org. Chem.* **1966**, *31*, 615.
(31) Jerchel, D.; Heider, J.; Wagner, H. *Liebigs Ann. Chem.* **1958**, *613*, 153.

Preparation of the Complexes. Pb(L⁵)(ClO₄)₂ (1). A solution of Pb(ClO₄)₂·4H₂O (0.072 g, 0.150 mmol) in absolute ethanol (5 mL) was added with stirring to a solution of [BaL⁵](ClO₄)₂ (0.136 g, 0.150 mmol) in the same solvent (35 mL). The reaction mixture was stirred and refluxed for 72 h. During the reaction the solution became turbid and a deep yellow precipitate appeared which was collected by filtration (yield 0.151 g (83%); mp 278 °C). Anal. Calcd for C₃₃H₄₁N₅O₁₂PbCl₂: C, 40.5; H, 4.2; N, 7.2. Found: C, 41.0; H, 4.0; N, 7.2. FAB-MS (*m/z*): 878 ([Pb(L⁵)(ClO₄)⁺], 779 ([Pb(L⁵)]⁺). IR (KBr): $\nu(\text{C}=\text{N})_{\text{imine}}$ 1635, $\nu(\text{C}=\text{N})_{\text{py}}$ 1585, $\nu_{\text{as}}(\text{Cl}-\text{O})$ 1088, $\delta_{\text{as}}(\text{O}-\text{Cl}-\text{O})$ 623 cm⁻¹. Λ_{M} (acetonitrile): 251 cm² Ω⁻¹ mol⁻¹ (2:1 electrolyte). Crystals suitable for X-ray crystallographic studies were grown by slow diffusion of diethyl ether into a solution of **1** in acetonitrile.

Pb(L⁵)(SCN)₂·2H₂O (2). *N,N'*-Bis(2-aminobenzyl)-4,13-diaza-18-crown-6 (0.059 g, 0.125 mmol) and Pb(SCN)₂ (0.033 g, 0.125 mmol) were dissolved in absolute ethanol. The mixture was stirred and heated while a solution of 2,6-diformylpyridine (0.017 g, 0.125 mmol) in absolute ethanol (40 mL) was added dropwise. After the addition was complete, the reaction mixture was stirred and refluxed for 24 h. The yellow solution was filtered while hot and the filtrate evaporated to 40 mL under vacuum. After the addition of diethyl ether a yellow precipitate appeared. It was collected by filtration and air-dried (yield 0.68 g (60%); mp 176 °C). Anal. Calcd for C₃₅H₄₁N₇O₄PbS₂·2H₂O C, 45.15; H, 4.9; N, 10.5. Found: C, 44.9; H, 4.6; N, 10.2. FAB-MS (*m/z*): 837 ([Pb(L⁵)(SCN)]⁺), 779 ([Pb(L⁵)]⁺). IR (KBr): $\nu(\text{C}=\text{N})_{\text{imine}}$ 1645, $\nu(\text{SCN})$ 2050 cm⁻¹. Λ_{M} (acetonitrile): 155 cm² Ω⁻¹ mol⁻¹ (1:1 electrolyte).

Pb₂(HL⁵)(NO₃)₅·2H₂O (3). 2,6-Diformylpyridine (0.042 g, 0.310 mmol) and Pb(NO₃)₂ (0.204 g, 0.620 mmol) were dissolved in acetonitrile (10 mL). The mixture was stirred and heated while a solution of *N,N'*-bis(2-aminobenzyl)-4,13-diaza-18-crown-6 (0.148 g, 0.310 mmol) in absolute ethanol (10 mL) was added dropwise. The reaction mixture was stirred and refluxed for 24 h and filtered while hot. The solution stood still for a few days and yellow crystals were formed, which were collected by filtration and air-dried (yield 0.116 g, 35%; mp 179–181 °C, dec). Anal. Calcd for C₃₃H₄₂N₁₀O₁₉Pb₂·2H₂O: C, 29.7; H, 3.5; N, 10.5. Found: C, 30.1; H, 3.2; N, 10.2. FAB-MS (*m/z*): 842 ([Pb(L⁵)(NO₃)⁺], 779 ([Pb(L⁵)]⁺). IR (KBr): $\nu(\text{C}=\text{N})_{\text{imine}}$ 1610, $\nu(\text{C}=\text{N})_{\text{py}}$ 1585, $\nu(\text{NO}_3)$ 1380 cm⁻¹. δ_{C} (solvent DMSO-*d*₆/CD₃CN, 295 K): 165.0, 163.3, 153.9, 153.7, 151.1, 142.1, 133.0, 132.6, 131.6, 131.5, 130.8, 130.2, 128.5, 127.7, 125.8, 121.3, 119.1, 69.3, 68.4, 68.1, 65.1, 58.6, 55.3. X-ray-quality crystals of formula [Pb(HL⁵)(NO₃)]₂[Pb(NO₃)₄] were grown by slow evaporation of the mother liquor.

Preparation of the Free Ligand: L⁵·2H₂O. A solution of [BaL⁵](ClO₄)₂ (0.3470 g, 0.0382 mmol) in chloroform was stirred with a water solution of guanidinium sulfate (0.4132 g, 0.1911 mmol) for 48 h. The organic phase was dried over MgSO₄, filtered, and concentrated in vacuo. The resulting yellow oil was treated with *n*-hexane and concentrated in vacuo. Compound L⁵·2H₂O was obtained as a yellow microcrystalline precipitate. It is air stable and soluble in chloroform (yield 0.1285 g, 65%; mp 78 °C). Anal. Calcd for C₃₃H₄₁N₅O₄·2H₂O: C, 65.2; H, 7.5; N, 11.5. Found: C, 64.9; H, 7.3; N, 11.1. FAB-MS (*m/z*): 518 ([L⁵H]⁺). IR (KBr, cm⁻¹): $\nu(\text{C}=\text{N})_{\text{imine}}$ 1628, $\nu(\text{C}=\text{N})_{\text{py}}$ 1585, $\nu(\text{C}=\text{C})$ 1601, 1595, $\delta(\text{CH}_2)$ 1451. δ_{H} (solvent CDCl₃, 295 K): 8.42 (2H, s, H_{imine}), 8.29 (2H, d), 8.00 (1H, t), 6.60–7.32 (8H, m), 3.9 (4H, m), 3.71 (16H, m), 2.55 (8H, m).

Physical Measurements. Elemental analyses were carried out on a Carlo Erba 1180 elemental analyzer, and FAB-MS were

recorded on a FISIONS QUATRO mass spectrometer with a Cs ion gun using 3-nitrobenzyl alcohol as matrix. High-resolution mass spectra using the electrospray ionizing technique were recorded on a Finnigan LCQ Advantage MAX. ¹H and ¹³C NMR spectra were run on a Bruker AC 200 F or a Bruker WM-500 spectrometer. ²⁰⁷Pb NMR natural abundance spectra were recorded at 298 K in the later spectrometer using a 10 mm VSP Bruker probe. Experiments were carried out in 0.02 M solutions of the complexes in 1:1 (w:w) CD₃CN/CH₃CN mixtures for internal lock. Chemical shifts are reported in parts per million from neat tetramethyllead using a saturated solution of Pb(Ph)₄ in CDCl₃ (−178 ppm) as external reference. IR spectra were recorded, as KBr disks, using a Bruker Vector 22 spectrophotometer. Conductivity measurements were carried out at 20 °C with a Crison Micro CM 2201 conductivimeter using 10⁻³ M solutions of the complexes in acetonitrile.

UV–vis spectra were recorded on Hewlett-Packard 8452A or Perkin-Elmer Lambda 900 spectrophotometers with quartz cuvettes (path length: 10 or 1 cm). The cell holder was thermostated at 25.0 °C, through circulating water. Protonation experiments of **1** were performed on 10⁻⁵ M solutions of **1** in MeCN (polarographic grade). Typically, aliquots of a fresh standard solution of trifluoroacetic acid were added and the UV–vis spectra of the samples were recorded. The formation of [Pb(L⁵)²⁺] was followed in a CH₃CN/CH₂Cl₂ (9:1, v:v) mixture. Typically an 8 × 10⁻⁶ M solution of the ligand was prepared and aliquots of a 1 × 10⁻³ M solution of Pb(ClO₄)₂·3H₂O were successively added. The spectrophotometric titration curves were fitted with the HYPERQUAD program.³³ Care was taken that in each titration, the *p* parameter (*p* = [concentration of complex]/[maximum possible concentration of complex]) was lower than 0.8, a condition required for the safe determination of a reliable equilibrium constant.³⁴

Crystal Structure Determinations. Three-dimensional X-ray data were collected at room temperature on a Bruker SMART 1000 CCD diffractometer by the ϕ – ω scan method. Reflections were measured from a hemisphere of data collected of frames each covering 0.3° in ω . Of the 47 830 (**1**) and 13 792 (**3**) reflections measured, all of which were corrected for Lorentz and polarization effects and for absorption by semiempirical methods based on symmetry-equivalent and repeated reflections, 5270 (**1**) and 5630 (**3**) independent reflections exceeded the significance level $|F|/\sigma(|F|) > 4.0$. Complex scattering factors were taken from the program package SHELXTL.³⁵ The structures were solved by direct methods and refined by full-matrix least-squares methods on *F*². The hydrogen atoms were included in calculated positions and refined by using a riding mode, except the hydrogen atom H(5N) for **3**, which was first located in a difference density map and then left to refine freely. Refinement converged with allowance for thermal anisotropy of all non-hydrogen atoms in all compounds. The crystal of **1** presents disorders on the ionic perchlorate and on several carbon atoms of the macrobicycle [site occupancy factors: 0.74(3) for O(11A) and O(12A) and 0.69(2) for C(15A) and C(16A)], and 132 restraints were imposed. The crystal of **3** also presents disorders on two carbon atoms, and 80 restraints had to be imposed [site occupancy factors: 0.55(4) for C(17A) and 0.613(18) for C(18A)]. Minimum and maximum final electronic density: −1.996 and 0.232 for **1** and −2.012 and 1.160 e Å⁻³ for

(33) Gans, P.; Sabatini, A.; Vacca, A. *Talanta* **1996**, *43*, 1739–1753.

(34) Wilcox, C. S. In *Frontiers in Supramolecular Chemistry and Photochemistry*; VCH: Weinheim, Germany, 1991; pp 123–143.

(35) Sheldrick, G. M. *SHELXTL: An Integrated System for Solving and Refining Crystal Structures from Diffraction Data (Revision 5.1)*; University of Göttingen: Göttingen, Germany, 1997.

Table 1. Crystal and Structure Refinement Data for **1** and **3**

param	1	3
formula	C ₃₃ H ₄₁ Cl ₂ N ₅ O _{12.5} Pb	C ₃₃ H ₄₂ N ₁₀ O ₁₉ Pb ₂
fw	977.80	1297.15
space group	<i>Pbca</i> (No. 61)	<i>P</i> $\bar{1}$ (No. 2)
cryst syst	orthorhombic	triclinic
<i>a</i> , Å	20.592(4)	10.5331(10)
<i>b</i> , Å	17.667(4)	13.8060(13)
<i>c</i> , Å	20.810(4)	14.8650(14)
α , deg	90	86.731(2)
β , deg	90	87.133(2)
γ , deg	90	81.359(2)
<i>V</i> , Å ³	7571(3)	2131.8(3)
<i>Z</i>	8	2
<i>T</i> , K	293(2)	293(2)
λ , Å (Mo K α)	0.710 73	0.710 73
<i>D</i> _{calcd} , g/cm ³	1.716	2.021
μ , mm ⁻¹	4.665	7.976
<i>R</i> ₁ ^a	0.0663	0.0467
<i>wR</i> ₂ (all data) ^a	0.1894	0.1148

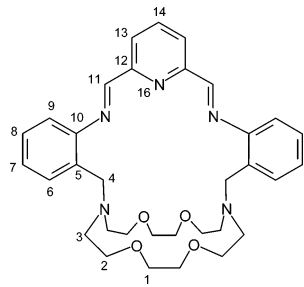
$$^a R_1 = \sum ||F_o| - |F_c|| / \sum |F_o|; wR_2 = \{ \sum [w(|F_o|^2 - |F_c|^2)]^2 / \sum [w(F_o^4)] \}^{1/2}.$$

3. Crystal data and details on data collection and refinement are summarized in Table 1.

Results and Discussion

Synthesis and Characterization. Compounds of formula Pb(L⁵)(SCN)₂·2H₂O (**2**) and Pb₂(HL⁵)(NO₃)₄·2H₂O (**3**) were easily prepared by a template Schiff-base condensation between the diamine precursor *N,N'*-bis(2-aminobenzyl)-4,13-diaza-18-crown-6 (L²) and 2,6-diformylpyridine in the presence of the appropriate lead(II) salt (thiocyanate or nitrate). Their FAB-mass spectra display peaks due to [Pb(L⁵)]⁺ (**2**) and [Pb(L⁵)(NO₃)]⁺ (**3**) at *m/z* (% BPI) = 779 (10) and 842 (47), respectively, that confirm that condensation and [1 + 1] cyclization has occurred and the lead(II) complexes were formed. This synthetic route does not work when perchlorate is the counterion of the lead(II) salt, giving a mixture of lead(II) complexes with the diamine precursor L² and the expected macrobicyclic L⁵. However, the compound of formula Pb(L⁵)(ClO₄)₂ (**1**) can be easily prepared by transmetalation of the barium derivative, Ba(L⁵)(ClO₄)₂, with lead(II) perchlorate. The FAB-mass spectrum of **1** features peaks due to [Pb(L⁵)(ClO₄)]⁺, *m/z* 878 (100% BPI), [Pb(L⁵)]⁺, *m/z* 779 (54% BPI), and [L⁵ + H]⁺, *m/z* 572 (24% BPI), and no peaks corresponding to species containing the [BaL⁵] fragment, providing initial evidence that the transmetalation reaction has indeed occurred and that the macrobicyclic L⁵ remains intact in the lead complex. The IR spectra of the three complexes present a band centered at ca. 1640 cm⁻¹ attributable to the $\nu(\text{C}=\text{N})_{\text{imine}}$ stretching mode and a band at ca. 1585 cm⁻¹ attributable to the $\nu(\text{C}=\text{N})_{\text{py}}$ stretching mode, together with bands corresponding to the anionic groups (perchlorate (**1**), thiocyanate (**2**), or nitrate (**3**)).

The ¹H and ¹³C NMR spectra of powdered samples **1** and **2** were recorded in CD₃CN solution (Table 2). The spectra of **1** were assigned on the basis of 2D H,H COSY, HMQC, and HMBC experiments, while those of **2** could be assigned by comparison with the spectra of **1**. The ¹³C spectra of both compounds display 14 signals for the 33 carbon atoms of

Table 2. ¹H and ¹³C NMR Data (δ , with respect to TMS) for Compounds **1** and **2**


¹ H	1 ^a	2 ^b	¹³ C	1 ^a	2
H1	3.52 (m), 16H ^c	2.40–4.00 (m), 28H	C1	68.0 ^c	68.7 ^c
H2					
H3					
H4					
H5	2.88 (s), 4H	7.38 (m), 8H ^c	C2	59.0	59.4
H6	3.57 (b), 2H		C3	57.0	54.7
H7	2.91 (s), 2H		C4		
H8			C5	131.1	131.3
H9	7.55 (m), 2H ^c	7.54 (t), 2H	C6	132.2	132.3
H10	7.36 (td), 2H		C7	128.1	127.9
H11	7.55 (m), 2H ^c		C8	130.5	130.5
H12	7.24 (d), 2H		C9	120.9	121.4
H13	9.10 (s), 2H	9.17 (s), 2H	C10	149.2	151.7
H14			C11	164.5	164.3
H15	8.30 (d), 2H	8.22 (d), 2H	C12	153.4	154.0
H16	8.56 (t), 1H	8.45 (t), 1H	C13	132.3	133.4
			C14	142.3	141.6

^a Conditions: assignment supported by 2D H,H COSY, HMQC, and HMBC experiments at 293 K, CD₃CN, 500 MHz. *J*_{14,13} = *J*_{13,14} = 7.74 Hz; *J*_{9,8} = 7.77 Hz; *J*_{7,8} = *J*_{8,6} = 7.47. ^b Conditions: *T* = 293 K, 200 MHz. ³*J*(¹H–²⁰⁷Pb) = 2.9 Hz; *J*_{14,13} = 7.32; *J*_{13,14} = 7.81 Hz; *J*_{9,8} = *J*_{8,7} = 7.32 Hz; *J*_{7,8} = *J*_{8,6} = 1.96 Hz. ^c Signals overlapped.

the ligand backbone, which indicates an effective C_{2v} symmetry for the complexes in solution with the lead(II) ion centered inside the cryptand cavity, in agreement with the solid-state structure of **1** (vide infra). The ¹H NMR spectra of **1** and **2** display a remarkable difference in the signal due to the imine protons H11, which appears as a singlet in both spectra but flanked by satellites attributable to proton coupling to the naturally abundant ²⁰⁷Pb (*I* = 1/2),³⁶ with a *J*(¹H–²⁰⁷Pb) = 2.9 Hz in the spectrum of **2**. This coupling reflects kinetic inertness in the complex, as well as a degree of covalence in the interaction between the lead(II) ion and the nearby donor atom. However, this coupling is relatively weak and much stronger couplings have been observed for other lead(II) complexes²⁸ with related ligands.

Crystals of compound **3** are poorly soluble in most of the common organic solvents, which has limited its study in solution. The ¹H NMR spectrum (200 MHz) obtained in a 2:1 (v:v) CD₃CN/DMSO-*d*₆ mixture features two signals for the imine protons [δ 9.23 (s, 1H), 8.94 (s, 1H)], which suggests an asymmetric coordination of the lead(II) ion inside the cryptand cavity, in agreement with the solid-state structure (vide infra). Asymmetric coordination of the lead(II) ion gives rise to the appearance of complicated multiplets in the aromatic region as well as overlapped broad signals in the region below δ = 4 ppm, which prevented a full assignment of the spectrum. The spectrum also displays a

(36) Bashall, A.; McPartlin, M.; Murphy, B. P.; Powell, H. R.; Waikar, S. *J. Chem. Soc., Dalton Trans.* **1994**, 1972.

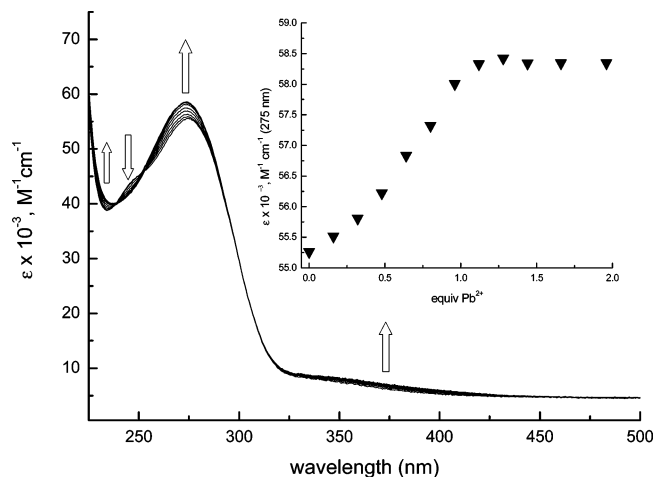
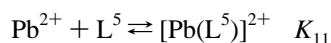
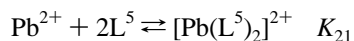


Figure 1. Family of spectra taken in the course of the titration of an MeCN/CH₂Cl₂ (9:1, v:v) solution 8×10^{-6} M in L⁵·2H₂O with a standard solution of Pb(ClO₄)₂·3H₂O at 25 °C. The titration profile is reported in the inset.

doublet at $\delta = 4.68$ (2H, $J = 5.4$ Hz) that we assign to the benzyl protons near the protonated bridgehead nitrogen atom. The ¹³C spectrum displays 17 and 6 signals for the 17 aromatic and 14 aliphatic carbon atoms of the ligand backbone, respectively, which suggests an effective C_s symmetry for the complex in solution, with the lead(II) ion noncentered inside the cryptand cavity.

To evaluate the binding ability of L⁵ toward lead(II), the free ligand was prepared by demetalation of the [Ba(L⁵)]²⁺ complex with guanidine sulfate. The complexation reaction of L⁵ with lead(II) perchlorate was followed by spectrophotometric titration experiments in CH₃CN/CH₂Cl₂ (9:1, v:v) mixtures since L⁵ is not soluble in acetonitrile. Figure 1 shows the family of spectra taken in the course of the titration. On addition of small aliquots of lead(II) perchlorate to a solution of free ligand, the intensity of the band at 275 nm and the shoulder at 350 nm progressively increase, while the shoulder at 245 nm decreases. The titration profile, presented in the inset of Figure 1, shows two inflection points for 2:1 and 1:1 (L⁵:Pb) stoichiometries, indicating the formation of at least two complex species in solution during the titration:



However, the curvature in the titration profile close to the 1:1 stoichiometry (Figure 1) is too steep to allow a safe determination of the binding constants, which is indicative of a high stability of the complex in solution. In particular, the p parameter ($p = [\text{concentration of complex}]/[\text{maximum possible concentration of complex}]$) was found to be higher than 0.8, a condition which does not permit the determination of a reliable equilibrium constant.³⁴ Analysis of the experimental data with a model including both 1:1 and 1:2 complex species allows us to estimate $\log K_{11} > 7$.

X-ray Crystal Structures. Slow diffusion of diethyl ether into a solution of **1** in acetonitrile gave X-ray-quality crystals of this compound. Crystals comprise the cation [Pb(L⁵)]⁺

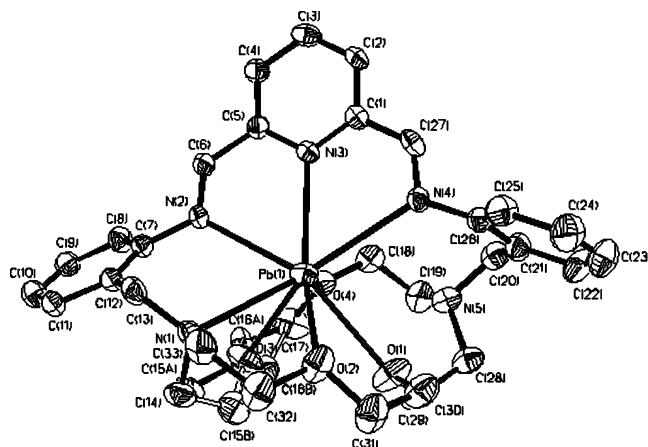


Figure 2. X-ray crystal structure of complex [Pb(L⁵)]²⁺ showing the atomic numbering scheme. The ORTEP plot is at the 30% probability level. Hydrogen atoms are omitted for simplicity.

and two perchlorate groups. One of these groups is well-separated from the cation, whereas the other seems to be weakly interacting with it, as suggested by the Pb–O(7) distance of 2.932(8) Å. Very often this weak interaction between a perchlorate group and a metal ion has been described as “semicoordination”,³⁷ and it is usually attributed to crystal packing forces in the solid state. Figure 2 displays a view of the structure of the cationic complex, while selected bond lengths and angles are given in Table 3. The lead(II) ion is eight-coordinate, and it places almost centered into the macrobicyclic cavity. The observed Pb(1)–N(5) distance (3.768(6) Å) clearly indicates that N(5) does not belong to the coordination sphere of the lead(II) ion. Likewise, the Pb–donor atoms bond lengths are ca. 0.1 Å longer than those found in its analogue with the smaller macrobicyclic L³,²⁷ which reflects a weaker interaction of the metal ion with L⁵ than with L³. These weaker interactions are the result of the centered position of the metal ion inside the macrobicyclic cavity, which presumably has been adopted to maximize interactions with the majority of the donor atoms of the receptor. This situation seems to be the result of two determinant features: the relatively large cavity of L⁵ in comparison with the size of Pb(II); the absence of donor groups with special greediness for this cation.

The fold of the macrobicyclic receptor around the metal ion lets donors N(1), N(5), O(4), and O(2) of the crown moiety be essentially coplanar (mean deviation from plane 0.022 Å). Dihedral angles N(3)–C(5)–C(6)–N(2), –4.3(11)°, and N(3)–C(1)–C(27A)–N(4), 4.2(11)°, indicate that the imine groups are not coplanar with the pyridine group. This planarity loss is related with the structure of the receptor and the coordinative requirements of the metal guest that force the receptor to fold increasing the stress of its structure. The lateral aromatic rings of L⁵ are in different planes, which intersect at 57.34(28)°. The plane of the pyridine ring forms dihedral angles of 50.25(26)° with the plane containing the benzyl ring bound to N(2) and 85.86(26)° with the plane containing the other aromatic ring. The distance between both

(37) Gowda, M. N.; Naikar, S. B.; Reddy, G. K. *Adv. Inorg. Radiochem.* **1984**, *28*, 255.

Table 3. Selected Bond Lengths (Å) and Angles (deg) for **1** and **3**

Compound 1			
Pb(1)–O(4)	2.696(5)	Pb(1)–O(2)	2.857(5)
Pb(1)–O(3)	2.704(6)	Pb(1)–N(2)	2.858(5)
Pb(1)–N(3)	2.824(5)	Pb(1)–N(1)	2.878(5)
Pb(1)–O(1)	2.836(6)	Pb(1)–N(4)	2.929(6)
O(4)–Pb(1)–O(3)	60.16(17)	O(2)–Pb(1)–N(2)	129.46(16)
O(4)–Pb(1)–N(3)	77.88(16)	O(4)–Pb(1)–N(1)	118.07(17)
O(3)–Pb(1)–N(3)	121.93(17)	O(3)–Pb(1)–N(1)	60.21(17)
O(4)–Pb(1)–O(1)	83.13(16)	N(3)–Pb(1)–N(1)	122.94(16)
O(3)–Pb(1)–O(1)	79.8(2)	O(1)–Pb(1)–N(1)	101.47(19)
N(3)–Pb(1)–O(1)	135.55(17)	O(2)–Pb(1)–N(1)	60.62(17)
O(4)–Pb(1)–O(2)	134.70(18)	N(2)–Pb(1)–N(1)	70.28(16)
O(3)–Pb(1)–O(2)	91.3(2)	O(4)–Pb(1)–N(4)	88.84(16)
N(3)–Pb(1)–O(2)	144.55(17)	O(3)–Pb(1)–N(4)	145.59(16)
O(1)–Pb(1)–O(2)	55.94(15)	N(3)–Pb(1)–N(4)	57.88(15)
O(4)–Pb(1)–N(2)	78.53(16)	O(1)–Pb(1)–N(4)	82.15(19)
O(3)–Pb(1)–N(2)	73.44(17)	O(2)–Pb(1)–N(4)	102.36(17)
N(3)–Pb(1)–N(2)	59.54(14)	N(2)–Pb(1)–N(4)	117.42(15)
O(1)–Pb(1)–N(2)	152.54(18)	N(1)–Pb(1)–N(4)	153.04(16)
Compound 3			
Pb(1)–O(7)	2.463(7)	Pb(1)–N(3)	2.685(6)
Pb(1)–N(2)	2.575(7)	Pb(1)–O(3)	2.725(6)
Pb(1)–N(1)	2.625(7)	Pb(1)–O(2)	2.745(6)
Pb(2)–O(13)	2.489(9)	Pb(2)–O(19)	2.708(7)
Pb(2)–O(8)	2.497(9)	Pb(2)–O(10)	2.733(9)
Pb(2)–O(14)	2.669(14)	Pb(2)–O(15)	2.746(11)
Pb(2)–O(12)	2.697(9)	Pb(2)–O(17)	2.859(9)
O(7)–Pb(1)–N(2)	73.9(2)	N(1)–Pb(1)–O(3)	64.3(2)
O(7)–Pb(1)–N(1)	76.9(2)	N(3)–Pb(1)–O(3)	119.0(2)
N(2)–Pb(1)–N(1)	77.6(2)	O(7)–Pb(1)–O(2)	82.0(2)
O(7)–Pb(1)–N(3)	73.8(2)	N(2)–Pb(1)–O(2)	139.7(2)
N(2)–Pb(1)–N(3)	64.3(2)	N(1)–Pb(1)–O(2)	65.6(2)
N(1)–Pb(1)–N(3)	136.8(2)	N(3)–Pb(1)–O(2)	138.0(2)
O(7)–Pb(1)–O(3)	133.7(2)	O(3)–Pb(1)–O(2)	102.6(2)
N(2)–Pb(1)–O(3)	74.0(2)	O(13)–Pb(2)–O(8)	76.5(3)
O(13)–Pb(2)–O(14)	78.5(4)	O(13)–Pb(2)–O(19)	72.8(2)
O(8)–Pb(2)–O(14)	79.5(4)	O(8)–Pb(2)–O(19)	140.7(3)
O(13)–Pb(2)–O(12)	48.5(3)	O(14)–Pb(2)–O(19)	116.8(4)
O(8)–Pb(2)–O(12)	71.5(3)	O(12)–Pb(2)–O(19)	69.9(2)
O(14)–Pb(2)–O(12)	123.5(4)	O(13)–Pb(2)–O(10)	112.5(3)
O(8)–Pb(2)–O(10)	47.8(3)	O(8)–Pb(2)–O(15)	119.8(4)
O(14)–Pb(2)–O(10)	116.2(4)	O(14)–Pb(2)–O(15)	43.0(5)
O(12)–Pb(2)–O(10)	76.4(3)	O(12)–Pb(2)–O(15)	120.8(3)
O(19)–Pb(2)–O(10)	126.6(2)	O(19)–Pb(2)–O(15)	75.6(3)
O(13)–Pb(2)–O(15)	76.3(3)	O(10)–Pb(2)–O(15)	157.3(4)
O(13)–Pb(2)–O(17)	101.3(3)	O(8)–Pb(2)–O(17)	121.1(3)
O(14)–Pb(2)–O(17)	159.1(4)	O(12)–Pb(2)–O(17)	65.7(2)
O(19)–Pb(2)–O(17)	45.3(2)	O(10)–Pb(2)–O(17)	83.4(2)
O(15)–Pb(2)–O(17)	116.3(4)		

imine nitrogen atoms (N(2) and N(4)) is 4.945(8) Å, whereas the distance between both pivotal nitrogen atoms (N(1) and N(5)) amounts to 6.353(9) Å.

Crystals of **3** contain two different structural units, the anion $[\text{Pb}(\text{NO}_3)_4]^{2-}$ and the cation $[\text{Pb}(\text{HL}^5)(\text{NO}_3)]^{2+}$. Figure 3a displays a view of the structure of the cation; selected bond lengths and angles are given in Table 3. Unlike **1**, now the lead(II) ion is clearly asymmetrically placed into the macrobicyclic cavity and only six-coordinated, bound to one imine nitrogen atom, N(2), one pivotal nitrogen atom, N(1), the pyridine nitrogen atom, N(3), and two oxygen atoms of the crown moiety, O(2) and O(3). The coordination sphere of the lead(II) ion is completed by an oxygen atom of a monodentate nitrate group. Neither nitrogen atoms N(5) and N(4) nor oxygen donors O(1) and O(4) belong to the lead(II) coordination environment, as evidenced by the observed Pb–donor distances [Pb(1)–N(5) 4.368(9); Pb(1)–N(4) 3.227(7); Pb–O(1) 3.085(7); Pb–O(4) 3.286(9) Å]. Moreover, this four donor atoms are involved in a so-called

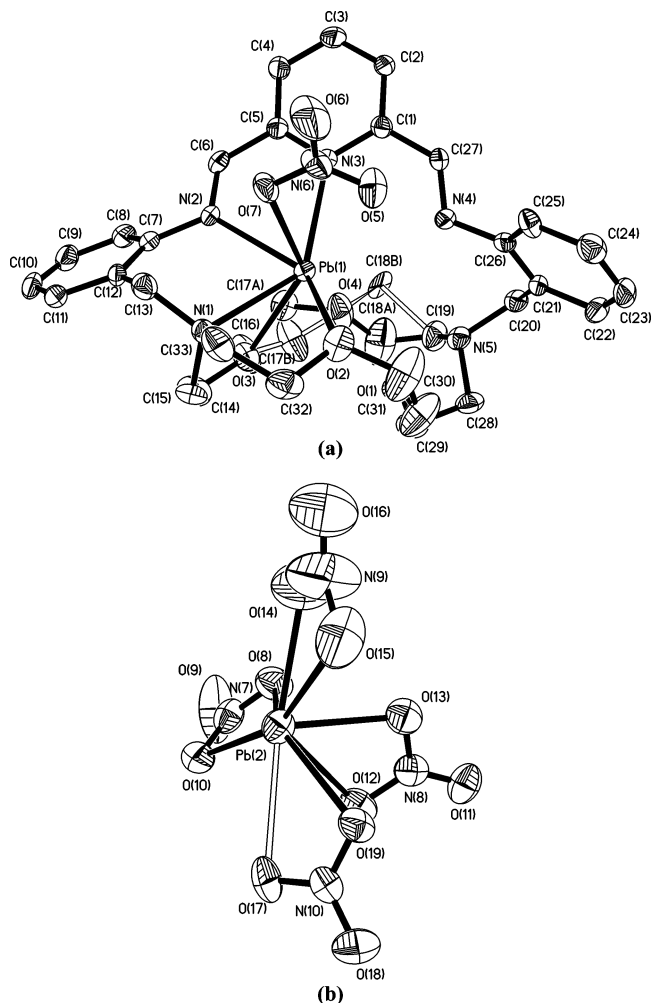


Figure 3. (a) X-ray crystal structure of complex $[\text{Pb}(\text{HL}^5)(\text{NO}_3)]^{2+}$ showing the atomic numbering scheme. The ORTEP plot is at the 30% probability level. Hydrogen atoms are omitted for simplicity. (b) X-ray crystal structure of complex $[\text{Pb}(\text{NO}_3)_4]^{2-}$ showing the atomic numbering scheme. The ORTEP plot is at the 30% probability level.

“multifurcated hydrogen bond”^{38–41} [N(5)⋯H(5N), 0.84(8) Å; N(5)⋯N(4) 3.134(11) Å, N(4)⋯H(5N) 2.50(7) Å, N(5)–H(5N)–N(4) 134(6)°; N(5)⋯O(1) 2.865(11) Å, O(1)⋯H(5N) 2.42(7) Å, N(5)–H(5N)–O(1) 114(6)°; N(5)⋯O(4) 2.793(11) Å, O(4)⋯H(5N) 2.44(7) Å, N(5)–H(5N)–O(4) 107(6)°]. The lateral aromatic rings of the protonated receptor (HL⁵)⁺ intersects at 70.19(31)°, whereas the plane of the pyridine ring forms dihedral angles of 54.53(26)° with the plane containing the benzyl ring bound to N(2) and of 71.78(27)° with the plane containing the other aromatic ring. Distances between both imine nitrogen atoms (N(2) and N(4), 5.032(10) Å) and between both pivotal nitrogen atoms (N(1) and N(5), 6.434(11) Å) are slightly longer than those found in $[\text{Pb}(\text{L}^5)(\text{ClO}_4)]^+$ where the receptor is not protonated. The second structural unit present in the crystals of **3**, $[\text{Pb}(\text{NO}_3)_4]^{2-}$, shows the lead(II) ion eight-coordinate, being bound to four

(38) Desiraju, G. R.; Steiner, T. *The Weak Hydrogen Bond*; Oxford University Press: New York, 1999.

(39) Steiner, T. *Crystallogr. Rev.* **1996**, *6*, 1.

(40) Steiner, T. *Angew. Chem., Int. Ed.* **2002**, *41*, 48.

(41) Elbasyouny, A.; Bruegge, H. J.; Von Deuten, K.; Knochel, A.; Koch, K. U.; Kopf, J.; Melzer, D.; Rudolph, G. *J. Am. Chem. Soc.* **1983**, *105*, 6568.

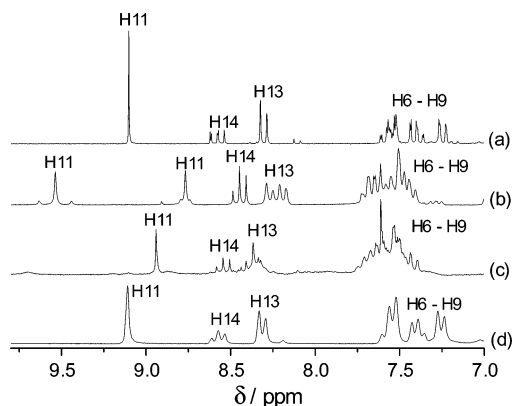


Figure 4. (a) Part of the 200 MHz ^1H NMR spectrum of **1** recorded in acetonitrile- d_3 at 293 K; (b) the spectrum of solution *a* upon addition of 1 equiv of trichloroacetic acid; (c) the spectrum of solution *a* after addition of 2 equiv of perchloric acid; and (d) the spectrum of solution *c* recorded upon addition of 2 equiv of triethylamine. See Table 2 for labeling scheme.

bidentated nitrate anions (Figure 3b). In light of the Pb–O bond lengths (Table 2), two of the interactions are strong (ca. 2.50 Å), three are moderate (ca. 2.70 Å), two are weak (ca. 2.74 Å), and the last one is very weak (2.859(9) Å). Two of the Pb–O bond lengths [Pb(2)–O(8) and Pb(2)–O(13)] are ca. 0.2 Å shorter than the remaining ones, and a void in the distribution of the ligands around the lead(II) ion is present (Figure 3b). This is typical of hemidirected lead(II) compounds in which the lead(II) lone pair is stereochemically active.⁴²

The asymmetrical position of the lead(II) ion in **3** is due to the presence of a proton on one pivotal nitrogen atom that is involved in hydrogen-bonding interaction with the contiguous imine nitrogen atom and one of the oxygen atoms of the crown moiety. The presence of that proton causes a translocation of the lead(II) ion into one end of the cavity of our receptor and a considerable modification of the coordination environment due to the blockade of some coordination sites and the electrostatic repulsion between the metal cation and the proton. This asymmetrical coordination environment around Pb(II) is very similar to that previously observed in $[\text{PbL}^6](\text{ClO}_4)_2$, where the phenol proton has been transferred to one of the imine nitrogen atoms being also involved in hydrogen-bonding interaction with the contiguous pivotal nitrogen atom.²⁸

Protonation Studies. The protonation of $\text{Pb}(\text{L}^5)(\text{ClO}_4)_2$ (**1**) has been followed by ^1H and ^{207}Pb NMR spectroscopy in CD_3CN and $\text{CD}_3\text{CN}/\text{D}_2\text{O}$ solutions and UV–vis spectroscopy in CH_3CN at 298 K. Figure 4 shows a part of the ^1H NMR spectrum of compound **1** recorded in CD_3CN solution prior addition of acid (Figure 4a) and after addition of 2 equiv of perchloric acid (Figure 4c). The spectrum shown in Figure 4c corresponds to a species with an effective C_{2v} symmetry in solution, and it is assigned to the diprotonated form of the free ligand $(\text{H}_2\text{L}^5)(\text{ClO}_4)_2$. This species has been previously isolated and characterized by single-crystal X-ray diffraction studies.⁴³ Thus, addition of 2 equiv of diluted perchloric acid to a solution of **1** leads to the

demetalation of the complex without macrobicyclic destruction. The demetalation process is fully reversible, and addition of 2 equiv of triethylamine to the latter solution causes deprotonation of the receptor and complexation of the removed lead(II) ion (Figure 4d). Both protonation and deprotonation processes caused by addition of perchloric acid and triethylamine, respectively, are very fast, and they hardly require more than a few minutes at room temperature. Protonation studies were also performed in $\text{CD}_3\text{CN}/\text{D}_2\text{O}$ (1:1) mixtures, showing a similar behavior, what also indicates that macrobicyclic **L**⁵ is inert toward hydrolysis under these conditions.

To step by step understand this demetalation process, we have also recorded the ^1H NMR spectra upon addition of only 1 equiv of acid. When 1 equiv of perchloric acid is added to a solution of **1**, the proton NMR spectrum features broad peaks that are due to the presence of exchange processes between different species in acetonitrile solution. Most likely this exchange process involves the presence of mono- and diprotonated species in solution. Addition of a weaker acid such as trichloro- or trifluoroacetic acid to a solution of **1** allowed us to identify a very interesting monoprotonated intermediate by NMR spectroscopy. Figure 4b displays the ^1H NMR spectrum after addition of 1 equiv of trichloroacetic acid, which is dramatically different from that of **1**. The signal due to the imine protons splits into two different signals appearing at 9.54 and 8.77 ppm, which is in agreement with an asymmetrical coordination of the lead(II) ion inside the macrobicyclic cavity as a consequence of the partial protonation of the receptor that decreases the effective symmetry of the complex in solution from C_{2v} to C_s . These two signals are flanked by satellites attributable to proton coupling to the naturally abundant ^{207}Pb ($I = 1/2$). The signal appearing at higher frequency presents a strong $J(^1\text{H}-^{207}\text{Pb})$ coupling (38.6 Hz), while for the peak at 8.77 ppm this coupling amounts to 10.7 Hz. This suggests that the imine group with proton NMR signal at 9.54 ppm coordinates stronger to the lead(II) ion than the other one. Likewise, the proton signal corresponding to proton H14 shifts upfield by 0.12 ppm, while the resonance due to protons H13 splits into two doublets that also shift to lower frequency, as expected for an effective C_s symmetry of the monoprotonated species in CD_3CN solution. Unfortunately, we have not obtained the X-ray crystal structure of this monoprotonated compound, but the X-ray crystal structure of compound **3**, where receptor **L**⁵ is also monoprotonated (vide supra), appears to be a good model for this intermediate. In **3**, the lead(II) ion is clearly asymmetrically placed into its cavity and the coordination number of Pb(II) has diminished with respect to that found in **1**, but much stronger interactions between the metal ion and the donor atoms of the receptor are now found, as evidenced by the short Pb–donor atom distances (Table 3). We have observed that when using trifluoroacetic acid, it is also possible to get a full demetalation of complex **1**, although an excess of acid and/

(42) Shimoni-Livny, L.; Glusker, J. P.; Bock, C. W. *Inorg. Chem.* **1998**, *37*, 1853.

(43) Avecilla, F.; Esteban, D.; Platas-Iglesias, C.; Fernández-Martínez, S.; De Blas, A.; Rodríguez-Blas, T. *Acta Crystallogr., Sect. C* **2005**, *C61*, o92.

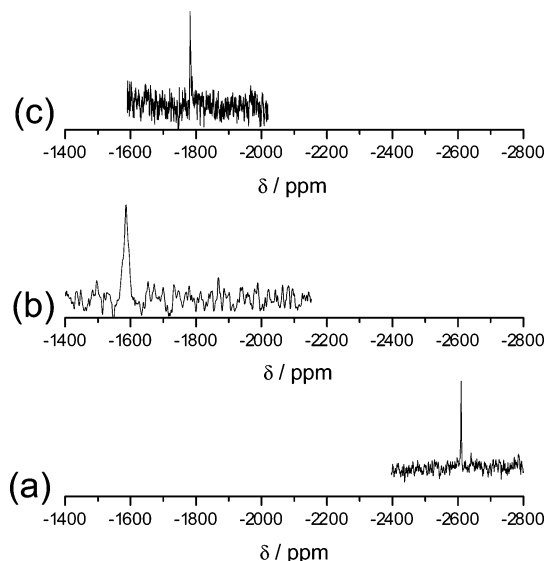


Figure 5. (a) 500 MHz ^{207}Pb NMR spectrum of **1** recorded in acetonitrile- d_3 at 293 K. (b) ^{207}Pb NMR spectrum of the same solution upon addition of 1 equiv of trichloroacetic acid. (c) 500 MHz ^{207}Pb NMR spectrum of $[\text{Pb}(\text{L}^3)](\text{ClO}_4)_2$ recorded under the same conditions.

or long reaction times (ca. 15 h) are now necessary. However, the use of a clearly weak acid such as trichloroacetic acid only allows monoprotection of **1**, being impossible to produce demetalation.

^{207}Pb NMR spectroscopy can provide useful insights into lead coordination chemistry. ^{207}Pb isotopes are particularly good candidates for nuclear magnetic resonance since they have a nuclear spin that can be exploited for NMR spectroscopy ($I = 1/2$), an excellent receptivity, a high natural abundance (22.6%), and a large chemical shift range (over 16 000 ppm).^{44,45} We therefore used ^{207}Pb NMR spectroscopy also to study the protonation of **1**. The results confirm those obtained from the ^1H NMR study. The ^{207}Pb NMR spectrum of **1** recorded at 298 K (Figure 5a) shows a rather sharp absorption peak at -2600 ppm ($w_{1/2} = 212$ Hz). This region is the typical for lead(II) salts (e.g., $\text{Pb}(\text{ClO}_4)_2 \cdot \text{H}_2\text{O}$),⁴⁶ in line with the weak coordination of lead(II) by the ligand in this complex evidenced by the solid-state structure. Upon addition of 1 equiv of trichloroacetic acid the resonance at -2600 ppm completely disappears, while a new relatively broad peak at -1583 ppm ($w_{1/2} = 1400$ Hz) is observed (Figure 5b). It has been shown that ^{207}Pb NMR chemical shifts move to lower fields in lead(II) poly(pyrazolyl)borate complexes as the coordination number of the metal ion decreases.⁴⁷ Moreover, the ^{207}Pb NMR spectrum of the related compound $[\text{Pb}(\text{L}^3)](\text{ClO}_4)_2$ (Figure 5), where the Pb–donor distances observed in the solid state are ca. 0.1 Å shorter than in **1**, shows a single sharp signal at -1782 ppm ($w_{1/2} = 243$ Hz). Thus, the large shift of the ^{207}Pb NMR

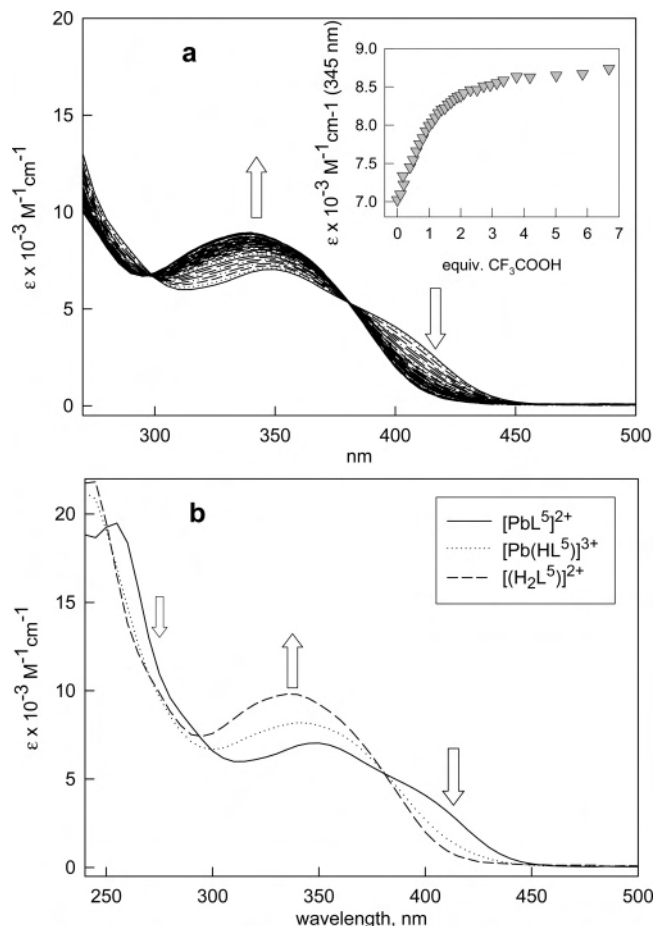


Figure 6. (a) Family of spectra taken in the course of the titration of an MeCN solution 10^{-3} M in **1** with a standard solution of CF_3COOH at 25 °C. The titration profile is reported in the inset. (b) Spectra of complex **1** recorded after addition of different amounts of CF_3COOH . The solid line refers to complex **1**, the dotted line to the spectrum of the same solution recorded 6 h after the addition of 1 equiv of acid, and the dashed line to that recorded 15 h after addition of 2 equiv of acid.

resonance to lower fields (ca. 1000 ppm) upon protonation of the ligand is in line with the lower coordination number and shorter Pb–donor distances observed in the solid state for **3** when compared to **1**.

Figure 6a shows the family of spectra taken in the course of the UV–vis titration of a solution of **1** in acetonitrile with trifluoroacetic acid. The UV–vis spectrum of **1** shows a broad band centered at 350 nm with a shoulder at 412 nm resulting from the $\pi \rightarrow \pi^*$ and $n \rightarrow \pi^*$ transitions on the aromatic subunits of the complex. Upon addition of trifluoroacetic acid, the intensity of the shoulder at 412 nm decreases, while the band at 350 nm experiment a blue shift while its intensity increases. The presence of two simultaneous isosbestic points at 298 and 381 nm indicates that only two species coexist at the equilibrium. The profile shown in the inset of Figure 6a indicates 1:1 stoichiometry for the monoprotinated intermediate. Data can be interpreted on the basis of the equilibrium $\mathbf{1} + \text{CF}_3\text{COOH} \rightleftharpoons [\mathbf{1}\cdot\text{H}]^+$, in which $[\mathbf{1}\cdot\text{H}]^+$ represents the monoprotinated intermediate. The curvature in the titration profile reported in inset a is according to the conditions to allow a safe determination of the binding constant. In particular, the p parameter ($p = [\text{concentration of complex}]/[\text{maximum possible concentration}]$

(44) Sanchiz, J.; Esparza, P.; Villagra, D.; Domínguez, S.; Mederos, A.; Brito, F.; Araujo, L.; Sánchez, A.; Arrieta, J. M. *Inorg. Chem.* **2002**, *41*, 6048.

(45) Claudio, E. S.; ter Horst, M. A.; Forde, C. E.; Stern, C. L.; Zart, M. K.; Godwin, H. A. *Inorg. Chem.* **2000**, *39*, 1391.

(46) Harrison, P. G.; Healy, M. A.; Steel, A. T. *J. Chem. Soc., Dalton Trans.* **1983**, 1845.

(47) Reger, D. L.; Huff, M. F.; Rheingold, A. L.; Haggerty, B. S. *J. Am. Chem. Soc.* **1992**, *114*, 579.

of complex]) was found to be lower than 0.8 and a reliable value of the monoprotation constant could be determined through nonlinear least-squares treatment of the titration profile: $\log K = 5.47 \pm 0.01$. Further addition of acid causes further changes in the UV spectra (Figure 6b) that did not permit one to calculate an equilibrium constant for the diprotonation process due to kinetic problems associated to the final demetalation process when trifluoroacetic acid is used. The spectrum of a solution of **1** recorded after 15 h of the addition of 2 equiv of this acid does not show further changes with time (Figure 6b). The high-resolution mass spectra using the electrospray ionizing technique of this solution confirm the presence of mono- and diprotonated forms in equilibrium.

Similar protonation studies were also carried out with the related and smaller receptor **L**³ (derived from 1,10-diaza-15-crown-5) and show that although addition of 2 equiv of perchloric acid to $[\text{Pb}(\text{L}^3)](\text{ClO}_4)_2$ also leads to the demetalation of the complex without receptor destruction, however, a long time (several weeks at room temperature) is necessary for the full demetalation of the complex. Likewise, in this case it has not been possible to stop the reaction in the intermediate step (after addition of only 1 equiv of acid). This different behavior shown by receptors **L**³ and **L**⁵ is explained by the different size of the macrobicyclic cavity in both receptors. The short Pb(II)–donor atom distances reported for the complex of **L**³ indicate a good fit of the receptor cavity and the metal ion guest,²⁷ which makes the demetalation of the complex by protonation of the receptor more difficult. On the other hand, the larger cavity size of **L**⁵ allows the metal ion to adopt different locations inside the macrobicyclic host.

Conclusions

The macrobicyclic receptor **L**⁵ derived from 4,13-diaza-18-crown-6 incorporating a pyridinyl Schiff-base spacer, forms stable complexes with lead(II) in the presence of different counterions. Thanks to the large cavity of this receptor and to the optimal distribution and nature of its donor atoms, the coordination of the guest lead(II) into the cavity of this receptor can be modulated by using external factors. So, the nature of the counterion present in the medium or the blockade of donor groups by protonation can

effectively control the coordination environment around the lead(II) ion. For instance, ¹H NMR spectroscopy points that the interaction between the Pb(II) ion and both imine nitrogen atoms becomes stronger when the two poorly coordinating perchlorate groups are replaced by thiocyanate groups. Indeed, the ¹H NMR spectrum of **2** displays the signal at $\delta = 9.16$ ppm corresponding to both imine protons flanked by satellites attributable to proton coupling to ²⁰⁷Pb, which is not observed in the spectrum of compound **1**. In solution, conductivity measurements suggest that at least one thiocyanate is bound to the metal ion, which probably causes the metal ion to be pushed out of the center of the cavity and brought nearer to both imine groups.

On the other hand, we have proved that **L**⁵ allows reversible complexation of lead(II). So, addition of 2 equiv of a strong acid such as diluted perchloric acid to a solution of the lead(II) complex leads to the demetalation of the complex without macrobicyclic destruction, which is recovered in its diprotonated form $(\text{H}_2\text{L}^5)(\text{ClO}_4)_2$. Studies performed with different acids show that the strength of the acid seems to be determinant in the rate of the demetalation process. This one happens very fast when perchloric acid is used, and it hardly requires more than just a few minutes at room temperature. This process is fully reversible, and the addition of 2 equiv of triethylamine to the resultant solution provokes deprotonation of the receptor and again complexation of the lead(II) ion. All of this, together with the fact that macrobicycle **L**⁵ is inert toward hydrolysis, opens very interesting perspectives for the use of this receptor as a new lead(II) extracting agent.⁴⁸

Acknowledgment. The authors thank A. Sánchez (Universidad de Santiago, Santiago, Spain) for the ²⁰⁷Pb NMR spectra recorded, H. Adams (University of Sheffield, Sheffield, U.K.) for the X-ray data collection of crystal **1**, and the Xunta de Galicia (Grant No. PGIDIT03TAM10301PR) for generous financial support.

Supporting Information Available: X-ray crystallographic files in CIF format for **1** and **3**. This material is available free of charge via the Internet at <http://pubs.acs.org>.

IC0482032

(48) Spain patent p200301940.